

# Triple-layer remote phosphor geometry: an excellent selection to improve the optical properties of white light-emitted diodes

Thuc Minh Bui<sup>1</sup>, My Hanh Nguyen Thi<sup>2</sup>, Nguyen Doan Quoc Anh<sup>3</sup>, Nguyen Le Thai<sup>4</sup>

<sup>1</sup>Faculty of Electrical and Electronics Engineering, Nha Trang University, Nha Trang City, Vietnam

<sup>2</sup>Faculty of Mechanical Engineering, Industrial University of Ho Chi Minh City, Ho Chi Minh City, Vietnam

<sup>3</sup>Faculty of Electrical and Electronics Engineering, Ton Duc Thang University, Ho Chi Minh City, Vietnam

<sup>4</sup>Faculty of Engineering and Technology, Nguyen Tat Thanh University, Ho Chi Minh City, Vietnam

## Article Info

### Article history:

Received Oct 3, 2020

Revised Apr 7, 2021

Accepted Apr 26, 2021

### Keywords:

Color rendering index

Dual-layer phosphor

Luminous efficacy

Mie-scattering theory

Triple-layer phosphor

## ABSTRACT

High performance white-light-emitting diodes (WLEDs) have been the goal of recent research on phosphor-in-glass (PiG) devices. In this paper, we introduce a configuration of WLED that achieves high color rendering index (CRI), and correlated color temperature with the addition of  $\text{Zn}_2\text{SiO}_4:\text{Mn}^{2+}$ ,  $\text{As}^{5+}$  and  $\text{YAl}_3\text{O}_4\text{B}_{12}:\text{Eu}^{3+}$ . The technique is lower the temperature during the creation process of phosphor in glass and control the consistent thickness in between 0.5 to 0.7 mm to yield high color quality PiG, high CRI above 80 WLEDs, and extend the color temperature range to 3,900 to 5,300 K. The consistent heat generation combined with extraordinary CRI for PiG prove that low temperature sintering has the potential to create WLEDs with advanced quality. The improved WLEDs can be utilized in many high-demand lighting fields such as chromatic examination, medical analysis, and aesthetic lighting.

This is an open access article under the [CC BY-SA](https://creativecommons.org/licenses/by-sa/4.0/) license.



## Corresponding Author:

Nguyen Le Thai

Faculty of Engineering and Technology, Nguyen Tat Thanh University

300A Nguyen Tat Thanh, Phuong 13, Quan 4, Thanh pho Ho Chi Minh 70000, Vietnam

Email: nlthai@nttu.edu.vn

## 1. INTRODUCTION

The white-light-emitting diodes (WLEDs) capable of converting white illumination from phosphor substances has been a desirable illumination means when it comes to lighting stability, durability, and eco-friendliness. As a result, this solid-state lighting solution began to replace older lighting methods and aim for more demanding lighting applications [1]–[3]. According to previous research results, the color rendering index is a key indicator to human perception of a light source, however, most WLEDs have a chroma rendition indicator (CRI) below 80 and only the highest quality can reach 80 as the consumer review in 2016 showed [4], [5]. So, to apply WLEDs in advanced lighting, the CRI must be above 90, which the current WLEDs fabricating method cannot obtain. To achieve this result, a solution of adding more phosphor materials ( $\text{Lu}_3\text{Al}_5\text{O}_{12}:\text{Ce}^{3+}$  and  $\text{CaAlSiN}_3:\text{Eu}^{2+}$ ) to produce constricted blue light spectrum, green, and red-light spectrum was introduced, which effectively create WLEDs with CRI over 90 [6]–[8]. As of late, phosphor-in-glass (PiG) WLEDs with CRI over 90 were shown on papers, however, the creation process, the optical properties, and materials set up to achieve such result have not been published [9], [10]. The PiG with stable heat performance in chromaticity coordinates shift and the ability to preserve lumen output in high energy apparatuses like laser exhibitor as well as laser illuminator [11]. Although there are many advantages in PiG, the temperature in which the PiG is crafted is the issue [12]–[14]. The 700 °C during the fabrication process of PiG creates an obscure area at the junction of the glass and red phosphor ( $\text{CaAlSiN}_3:\text{Eu}^{2+}$ ) and induce inter-diffusion between these materials. Besides, the high temperature during sinister cause the

emitted light and transparency of the red PiG to decrease, which is detrimental to the CRI of PiG making the PiG unsuitable for high-demand lighting applications as it is required by international commission on illumination (CIE) that the appropriate WLEDs must reach 90 in CRI [15]–[17]. Considering these circumstances, improving the CRI of co-doped PiG by adjusting temperature in the sintering process is an essential step to enhance the WLED.

To achieve high CRI co-doped PiG,  $\text{Zn}_2\text{SiO}_4:\text{Mn}^{2+}$ ,  $\text{As}^{5+}$  and  $\text{YAl}_3\text{O}_4\text{B}_{12}:\text{Eu}^{3+}$  were distributed on the glass matrix ( $\text{B}_2\text{O}_3\text{-Sb}_2\text{O}_3\text{-SiO}_2\text{-Ta}_2\text{O}_5$ ). Before conducting the experiments, the sintering temperature and refractive index need to be adjusted by balancing the percentage of  $\text{B}_2\text{O}_3$  and  $\text{SiO}_2$  glass components. On the other hand, the glass matrix also received adjustments through  $\text{Sb}_2\text{O}_3$  and  $\text{Ta}_2\text{O}_5$  for the purpose of eliminating gaseous contents as well as attaining significant refraction indicator. The correct procedure to produce glass matrix is to start by mixing the ingredients evenly, then baked at  $1,080^\circ\text{C}$ , and leave to rest in normal air temperature. The calculation outcomes suggest that the glass matrix has good lighting transparency, significant refraction indicator reaching 1.8, exhibits the glass shift heat level of  $527^\circ\text{C}$ , and thawing heat level reaching  $593^\circ\text{C}$ . As a result, glass matrix with  $\text{Sb}_2\text{O}_3$  and  $\text{Ta}_2\text{O}_5$  is optimal for dually-incorporated PiG, able to reach significant CRI chroma transmutation sheet applicable to demanding interior illuminating utilization. Low sintering temperature that is employed for lessening cross-dispersion among the materials from the dually-incorporated PiG WLED apparatuses yielding CRI=94 will be illustrated. First, the green as well as red phosphor samples are diffused onto the glass latticework. Afterwards, the sintering heat level, fraction as well as mass proportion for said samples would receive appropriate adjustment, completing the goal of high CRI. Though dually-incorporated PiG thickness management, the correlated chroma temperatures (CCTs) in the WLED apparatuses would be between 3,900 and 5,300 K. The innovative co-doped PiG with great heat generation consistency can be the solution for WLEDs with optic attributes suiting demanding illumination purposes.

## 2. RESEARCH METHOD

### 2.1. Preparation of phosphor materials

The following section will demonstrate the process to obtain the phosphor materials used in our experimental tests. The starting materials would be  $\text{Zn}_2\text{SiO}_4:\text{Mn}^{2+}$ ,  $\text{As}^{5+}$ . The constituents for this green substance would be blended by milling within water for 2 hours. After the ingredients are mixed into one mixture, leave it to dry. Once the compound is dry, grind it into powder. The final step is placing the powder from the last process within a closed quartz tube then firing under  $1,200^\circ\text{C}$  within an hour. The final substance should emit green color and has a discharge apex reaching 2.35 eV. The Table 1 displays the chemical constituents that create the  $\text{Zn}_2\text{SiO}_4:\text{Mn}^{2+}$ ,  $\text{As}^{5+}$  phosphor [18].

The red phosphor  $\text{YAl}_3\text{B}_4\text{O}_{12}:\text{Eu}^{3+}$  fabricated through 6 steps: mixing, 4 consecutive firing steps, and washing. Like green phosphor, the ingredients of red phosphor would be blended via pulverizing. Secondly, put the compound within unclosed quartz boats and fire within sixty minutes at  $500^\circ\text{C}$ , the substance from this step will be grinded into powder before moving on to the next step. The next three steps are the compound being placed on open alumina crucibles and fire for 1 hour under  $900$ ,  $1,100$ , and  $1,200^\circ\text{C}$ . The product will be grinded to attain powder when the firing process is finished. Following the final heating step, clean the final substance in boiling water for multiple instances to remove residue then leave it till dry. The completed red  $\text{YAl}_3\text{B}_4\text{O}_{12}:\text{Eu}^{3+}$  phosphor will have red emission color and 2.01 and 2.035 eV emission peaks. The chemical composition is shown in Table 2 [19].

Table 1. Constituents for  $\text{Zn}_2\text{SiO}_4:\text{Mn}^{2+}$ ,  $\text{As}^{5+}$

Constituent	Mole %	Mass (g)
ZnO	200	163
MnCO <sub>3</sub>	0.2	0.230
SiO <sub>2</sub>	102	62.1
As <sub>2</sub> O <sub>3</sub>	0.02 (of As)	0.02

Table 2. Constituents for  $\text{YAl}_3\text{B}_4\text{O}_{12}:\text{Eu}^{3+}$

Constituents	Mole %	Mass (g)
Y <sub>2</sub> O <sub>3</sub>	90 (of Y)	102
Eu <sub>2</sub> O <sub>3</sub>	10 (of Eu)	17.6
Al <sub>2</sub> O <sub>3</sub>	300 (of Al)	153
H <sub>3</sub> BO <sub>3</sub>	410	248

### 2.2. Recreation

Figure 1 displays the organization inside a WLED utilized in our research. Figures 1(a) and 1(b) show there are remote half dome to cover below, a remote-plate, and a conformal-coating pc-WLED package. The blue area at the base is the blue light-emitting diodes (LEDs), the chromatic plate are the phosphor materials, and the unoccupied zones between the plates and silicone. The substrate is aluminum nitride. The yellow phosphor would be  $\text{YAG}:\text{Ce}^{3+}$ .  $5,600\text{ K}$  is the default color temperature for all structures when observing along the z-axis.

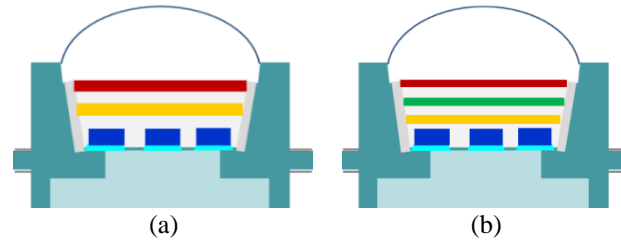


Figure 1. Multi-sheet settings for WLED (a) double-sheet phosphor (DL) and (b) three-sheet (TL)

Each phosphor plate is limited to 0.08 mm in density, guaranteeing precise calculation data. The concentration of yellow  $\text{YAG:Ce}^{3+}$  also has an important role in which it must be changed accordingly to other chromatic phosphor proportions. This is to prevent the color temperature of WLED from changing and affect the results of experiments. The  $\text{YAG:Ce}^{3+}$  content within the settings and average correlated color temperatures (ACCT) [20] will have disparate amount and that results in the diversity of scattering and optical properties of WLEDs.

In Figures 2(a) and 2(b), the  $\text{YAG:Ce}^{3+}$  concentration in DL and TL are compared, which leads to the results that DL at all ACCTs will have higher amount of yellow phosphor. More yellow phosphor at all ACCTs means the light emission capacity is reduced due to the back-scattering effect. In addition, the color quality is also damaged as the balance between the primary colors contributes to white light is distorted because the yellow phosphor increases. Therefore, the reduction of back-scattering, luminous flux enhancement, and chromatic performance improvement are the obstacles when enhancing WLEDs, which can be solved by adding the red and green phosphor to enforce control with the extra chromatic light components. Considering these requirements, the three-sheet configuration appears to be a good solution. To verify this theory, other optical properties are examined for reference. Figure 3 displays the discharge spectra of each setting across a range of wavelengths. The spectra intensity in the TL setting noticeably surpasses that in the DL setting, indicating greater proficiency from the TL setting.

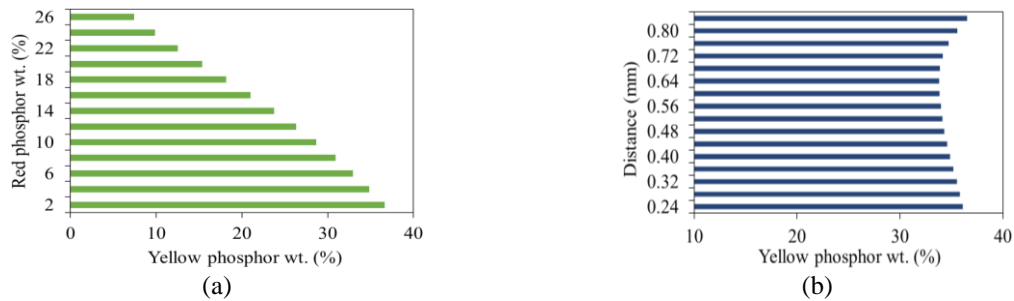


Figure 2.  $\text{YAG:Ce}^{3+}$  content within all settings (a) DL and (b) TL

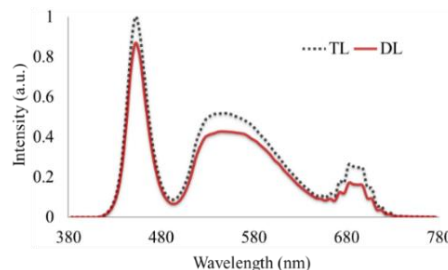


Figure 3. Discharge spectra in the settings

### 3. RESULTS AND DISCUSSION

The color rendering index between dual-layer and triple-layer are examined side by side in Figures 4(a) and 4(b). The resulted CRI from DL is certainly higher than TL at all ACCTs. The CRI in DL

keeps increase as the color temperature rises and reach it peak at 8,500 K. Considering how hard achieving good CRI in WLEDs with color temperature higher temperature higher than 7,000 K is, this finding in DL structure makes it the optimal choice for WLEDs that aim for high CRI. The high CRI in DL is resulted from  $YAl_3O_4B_{12}:Eu^{3+}$  added into the structure, which certifies DL as the structure with best CRI even greater than TL structure. This result shows that DL can be effective if employed in the production process to create WLEDs with high CRI. However, CRI is not the only quality indicator that is important to the WLEDs quality evaluation. In fact, many researchers have utilized color quality scale (CQS) instead CRI due to CRI having limited evaluation scope while CQS including CRI, viewers' preference, and chromaticity coordinate is much more valuable. The CQS of the structures applied in this research are determined then displayed by Figure 5. Contrary to CRI, the CQS from TL is higher than DL as the TL is benefited by 3 different chromatic phosphor layers. The results from Figure 5 prove that if the color quality is what the manufacturers are after, the TL structure is the suitable option. However, in WLEDs with advanced chromatic performance, the light output usually is damaged in the process. So, is the light output in triple-layer remote phosphor also negatively impacted as side effect of good color quality? the luminous flux of both TL and DL must be compared to clarify this question. Therefore, the next part will demonstrate the calculation equations used to estimate propagated blue illumination as well as transmuted yellow illumination within the three-sheet setting.

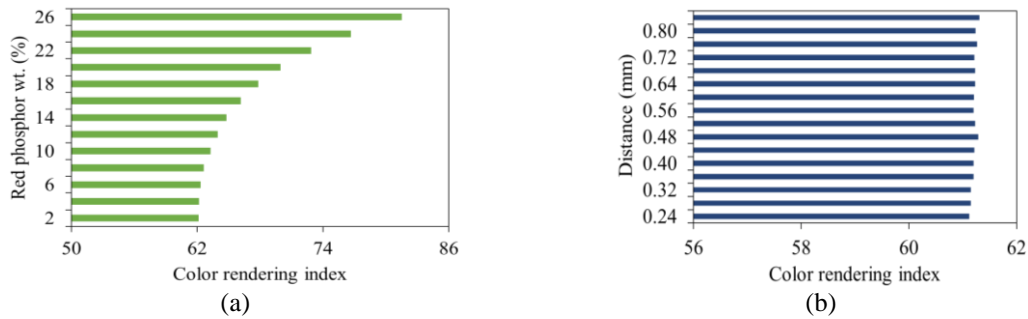


Figure 4. CRI in all settings corresponding to ACCT levels (a) DL and (b) TL

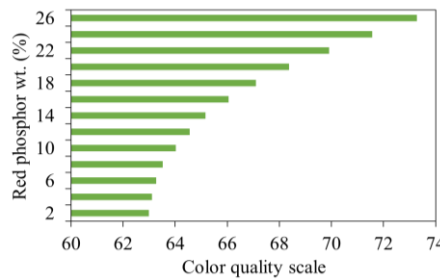


Figure 5. CQS in all settings corresponding to ACCT levels

Various computational expressions were utilized to assess the illumination mechanism in each setting. The transmitted blue illumination and converted yellow illumination in the case of double-sheet phosphor setting having the phosphor sheet breadth ( $h$ ) would be expressed as formulas (1) and (2) [21]–[23]. The propagated blue illumination as well as transmuted yellow illumination in the case of three-sheet setting having phosphor sheet breadth reaching  $\frac{2}{3}$  would be assessed via the formulas (3) to (5):

$$PB_2 = PB_0 e^{-\alpha_{B_2} h} e^{-\alpha_{B_2} h} = PB_0 e^{-2\alpha_{B_2} h} \tag{1}$$

$$PY_2 = \frac{1}{2} \frac{\beta_2 PB_0}{\alpha_{B_2} - \alpha_{Y_2}} [e^{-\alpha_{Y_2} h} - e^{-\alpha_{B_2} h}] e^{-\alpha_{Y_2} h} + \frac{1}{2} \frac{\beta_2 PB_0}{\alpha_{B_2} - \alpha_{Y_2}} [e^{-\alpha_{Y_2} h} - e^{-\alpha_{B_2} h}] \tag{2}$$

$$= \frac{1}{2} \frac{\beta_2 PB_0}{\alpha_{B_2} - \alpha_{Y_2}} [e^{-2\alpha_{Y_1} h} - e^{-2\alpha_{B_1} h}]$$

$$PB_3 = PB_0 \cdot e^{-\alpha_{B_2} \frac{2h}{3}} \cdot e^{-\alpha_{B_2} \frac{2h}{3}} \cdot e^{-\alpha_{B_2} \frac{2h}{3}} = PB_0 \cdot e^{-2\alpha_{B_3} h} \tag{3}$$

$$\begin{aligned}
 PY'_3 &= \frac{1}{2} \frac{\beta_3 PB_0}{\alpha_{B_3} - \alpha_{Y_3}} \left[ e^{-\alpha_{Y_3} \frac{2h}{3}} - e^{-\alpha_{B_3} \frac{2h}{3}} \right] e^{-\alpha_{Y_3} \frac{2h}{3}} + \frac{1}{2} \frac{\beta_3 PB_0 e^{-\alpha_{B_3} \frac{2h}{3}}}{\alpha_{B_3} - \alpha_{Y_3}} \\
 &\quad \left[ e^{-\alpha_{Y_3} \frac{2h}{3}} - e^{-\alpha_{B_3} \frac{2h}{3}} \right] \\
 &= \frac{1}{2} \frac{\beta_3 PB_0}{\alpha_{B_3} - \alpha_{Y_3}} \left[ e^{-\alpha_{Y_3} \frac{4h}{3}} - e^{-2\alpha_{B_3} \frac{4h}{3}} \right]
 \end{aligned} \tag{4}$$

$$\begin{aligned}
 PY_3 &= PY'_3 \cdot e^{-\alpha_{Y_3} \frac{2h}{3}} + PB_0 \cdot e^{-2\alpha_{B_3} \frac{4h}{3}} \frac{1}{2} \frac{\beta_3}{\alpha_{B_3} - \alpha_{Y_3}} \left[ e^{-\alpha_{Y_3} \frac{2h}{3}} - e^{-\alpha_{B_3} \frac{2h}{3}} \right] \\
 &= \frac{1}{2} \frac{\beta_3 PB_0}{\alpha_{B_3} - \alpha_{Y_3}} \left[ e^{-\alpha_{Y_3} \frac{4h}{3}} - e^{-\alpha_{B_3} \frac{4h}{3}} \right] e^{-\alpha_{Y_3} \frac{2h}{3}} + \frac{1}{2} \frac{\beta_3 PB_0 e^{-\alpha_{B_3} \frac{4h}{3}}}{\alpha_{B_3} - \alpha_{Y_3}} \\
 &\quad \left[ e^{-\alpha_{Y_3} \frac{2h}{3}} - e^{-\alpha_{B_3} \frac{2h}{3}} \right] \\
 &= \frac{1}{2} \frac{\beta_3 PB_0}{\alpha_{B_3} - \alpha_{Y_3}} \left[ e^{-\alpha_{Y_3} h} - e^{-2\alpha_{B_3} h} \right]
 \end{aligned} \tag{5}$$

$h$  signifies the phosphor sheet's breadth. The subscripts "1" as well as "2" signify double-sheet as well as triple-sheet structures.  $\beta$  signifies the transmutation coefficient applying to blue illumination transmuting into yellow illumination.  $\gamma$  signifies the reflectivity coefficient for yellow illumination. The intenseness for blue ( $PB$ ) as well as yellow illumination ( $PY$ ) would be the illumination intenseness generated by blue LED, signified via  $PB_0$ .  $\alpha_B$ ,  $\alpha_Y$  signify the fractions for the power penalty applying to blue and yellow illumination when being propagated within the phosphor sheet. Besides, in subscript "4",  $PY'_3$  signifies the propagated yellow illumination bypassing the pair of phosphor sheets. In the case of three-sheet structure, the illumination proficiency for pc-LED device would be augmented substantially compared to the two-sheet variant [24]. As such, it could become the preferred structure in WLEDs. The formula below demonstrates the superiority of proficiency in the three-sheet setting to that in the double-sheet setting.

$$\frac{(PB_3 - PY_3) - (PB_2 + PY_2)}{(PB_2 + PY_2)} > \frac{e^{-2\alpha_{B_3} h} - e^{-2\alpha_{B_2} h}}{e^{-2\alpha_{Y_3} h} - e^{-2\alpha_{B_2} h}} \tag{6}$$

Mie hypothesis will be employed for assessing phosphor granules' dispersion. Additionally, via a formula derived from said hypothesis, we can determine the dispersion cross section  $C_{sca}$  applying to globular granules. It is possible to determine the propagated illumination energy via the Lambert-Beer principle [25]:

$$I = I_0 \exp(-\mu_{ext} L) \tag{7}$$

$I_0$  signifies the incident illumination energy.  $L$  signifies the phosphor sheet breadth (mm).  $\mu_{ext}$  signifies the extinction coefficient, equal to  $N_r C_{ext}$ , with  $N_r$  signifying the number denseness allocation for granules ( $\text{mm}^{-3}$ ).  $C_{ext}$  ( $\text{mm}^2$ ) signifies the extinction cross-section for phosphor granules.

From (6), it can be concluded that more phosphor layers do not harm the lumen output of the device, on the contrary, the emitted light from TL is higher than DL. Figure 6, which demonstrates the calculated flux of TL and DL, can be viewed for better understanding with Figures 6(a) and 6(b) displaying the lumen output in the DL and TL settings, respectively. The lumen output in the TL setting surpasses that in the DL setting in certain zones. Thus, the TL structure is the configuration that can achieve high CQS while maintaining the emitted light at a high amount. This result is yielded from the more enhanced emission rate from 500 to 600 nm wavelength in TL structure because the yellow phosphor concentration in this structure is reduced, thus sustaining ACCT. From these circumstances, the TL setting reduce the illumination loss from internal reflection and let the emitted light from blue light source to move through phosphor layers more effectively, which can also be known as allow the light conversion to occur more effective. The TL structure, with higher emission intensity in the spectrum will achieve better results in terms of light output.

Besides other optical properties, the chromatic consistency of emitted light is also an important index that needs attention. There are many solutions to enhance the color uniformity from using conformal coating method to adding phosphor particles such as  $\text{SiO}_2$ , and  $\text{CaCO}_3$ . These solutions are effective regarding the primary goal of improving color uniformity, however, the light output is also reduced. On the other hand, applying both  $\text{Zn}_2\text{SiO}_4:\text{Mn}^{2+}$ ,  $\text{As}^{5+}$  and  $\text{YAl}_3\text{O}_4\text{B}_{12}:\text{Eu}^{3+}$  into the structure augmented the chroma proficiency through scattering particles as well as boosting light emission. The remote phosphor configuration of the TL structure is also another advantage because the gap between the phosphor plates can lower the back-scattering event. The Lambert-Beer principle displayed by (7) proves that the concentrations for the phosphor materials still need to be adjusted in order to achieve the best result. Looking at the

variations of color expression of both DL and TL in Figure 7, we can see that TL offers superior color consistency to DL because the color deviation of TL is lower, and the discrepancy become more significant towards higher color temperature such as 8,500 K. This is because the TL has more phosphor layers, which will generate more scattering events that support the chromatic consistency of emitted light. However, more scattering events also means more light loss due to back-scattering. However, the reduction in light emission can be omitted considering the advantages that TL brings to WLEDs, and how the TL manages to achieve highest performance in both chromatic performance and light output.

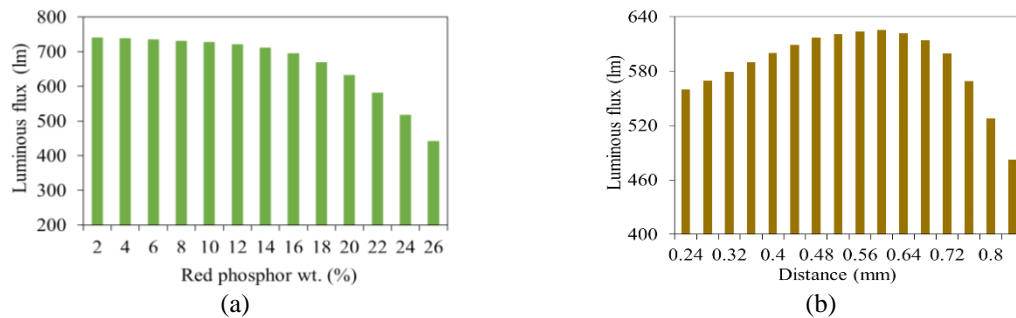


Figure 6. Lumen proficiency in all settings corresponding under various ACCT values (a) DL and (b) TL

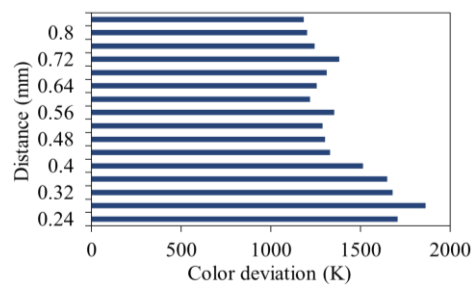


Figure 7. Correlated chroma temperature aberration (D-CCT) in all settings under various ACCT values

#### 4. CONCLUSION

In conclusion, the method of lowering the temperature during fabrication procedure to create WLEDs with high CRI and diverse correlated color temperature from 3,900 to 5,300 K were shown and discussed. Lowering the sintering temperature 620 °C for the purpose of limiting the cross-dispersion among the red phosphor as well as glass yielded high CRI. The CRI from WLEDs that follow this method can surpass the highest result, which is 80 as demonstrated by previous studies. This co-doped PiG that can adapt to multiple difficult demands of the lighting industry can be a potential solution for higher performance lighting devices that are enhanced in optical properties and suitable for advanced lighting applications.

#### REFERENCES

- [1] S. Liang, Y. Jia, Z. Qin, and H. Sun, "Influences of nutrient concentration of overlying water on nitrogen and phosphor release from sediment in Lake Baiyangdian," in *2011 International Conference on Remote Sensing, Environment and Transportation Engineering*, Jun. 2011, pp. 2225–2228. doi: 10.1109/RSETE.2011.5964751.
- [2] P. S. Reddy, R. A. R. Kumar, M. G. Mathews, and G. Amarendra, "Remote online performance evaluation of photomultiplier tube and electronics of DPCAM," *IEEE Transactions on Nuclear Science*, vol. 64, no. 11, pp. 2843–2853, Nov. 2017, doi: 10.1109/TNS.2017.2760891.
- [3] F. Zhao, G. Dong, G. Yang, Y. Zeng, B. Shieh, and S. W. Ricky Lee, "Study on light emitting surface temperature of LEDs," *21st International Conference on Electronic Packaging Technology (ICEPT)*, 2020, pp. 1–5. doi: 10.1109/ICEPT50128.2020.9202667.
- [4] P. C. Acuna, S. Leyre, J. Audenaert, Y. Meuret, G. Deconinck, and P. Hanselaer, "Impact of the geometrical and optical parameters on the performance of a cylindrical remote phosphor LED," *IEEE Photonics Journal*, vol. 7, no. 5, pp. 1–14, 2015, doi: 10.1109/JPHOT.2015.2468679.
- [5] J.-S. Li, Y. Tang, Z.-T. Li, J.-X. Chen, X.-R. Ding, and B.-H. Yu, "Precise optical modeling of phosphor-converted LEDs with arbitrary concentration and thickness using bidirectional scattering distribution function," *IEEE Photonics Journal*, vol. 10, no. 5, pp. 1–17, 2018, doi: 10.1109/JPHOT.2018.2866864.

- [6] C.-C. Sun *et al.*, “Spatial-coded phosphor coating for high-efficiency white LEDs,” *IEEE Photonics Journal*, vol. 9, no. 3, pp. 1–9, Jun. 2017, doi: 10.1109/JPHOT.2017.2703129.
- [7] S. D. Alaruri, A. J. Brewington, M. A. Thomas, and J. A. Miller, “High-temperature remote thermometry using laser-induced fluorescence decay lifetime measurements of  $Y_2O_3:Eu$  and  $YAG:Tb$  thermographic phosphors,” *IEEE Transactions on Instrumentation and Measurement*, vol. 42, no. 3, pp. 735–739, Jun. 1993, doi: 10.1109/19.231599.
- [8] D.-C. Chen, Z.-G. Liu, Z.-H. Deng, C. Wang, Y.-G. Cao, and Q.-L. Liu, “Optimization of light efficacy and angular color uniformity by hybrid phosphor particle size for white light-emitting diode,” in *2013 10th China International Forum on Solid State Lighting (ChinaSSL)*, Nov. 2013, pp. 95–99. doi: 10.1109/SSLCHINA.2013.7177322.
- [9] E. Juntunen, O. Tapaninen, A. Sitomaniemi, and V. Heikkinen, “Effect of phosphor encapsulant on the thermal resistance of a high-power COB LED module,” *IEEE Transactions on Components, Packaging and Manufacturing Technology*, vol. 3, no. 7, pp. 1148–1154, Jul. 2013, doi: 10.1109/TCPMT.2013.2260796.
- [10] C.-T. Li and Y. Li, “Color-decoupled photo response non-uniformity for digital image forensics,” *IEEE Transactions on Circuits and Systems for Video Technology*, vol. 22, no. 2, pp. 260–271, Feb. 2012, doi: 10.1109/TCSVT.2011.2160750.
- [11] L. Liu, X. Tan, D. Teng, M. Wu, and G. Wang, “Simultaneously enhancing the angular-color uniformity, luminous efficiency, and reliability of white light-emitting diodes by  $ZnO@SiO_2$  modified silicones,” *IEEE Transactions on Components, Packaging and Manufacturing Technology*, vol. 5, no. 5, pp. 599–605, 2015, doi: 10.1109/TCPMT.2015.2424981.
- [12] M.-R. Shin, R. Moon, J.-Y. Lee, and Y.-J. Kim, “Proposal and design of hybrid light guide plate for large-area LED display to improve illuminance and color uniformity,” in *Technical Digest of the Eighteenth Microoptics Conference*, 2013, pp. 1–2.
- [13] J. Zou, F. Han, Z. Zhang, H. Zheng, S. Liu, and S. Liu, “Fabrication of phosphor pillar based on electrohydrodynamic for high angular color uniformity of white light-emitting diodes,” in *2018 19th International Conference on Electronic Packaging Technology (ICEPT)*, 2018, pp. 1421–1425. doi: 10.1109/ICEPT.2018.8480503.
- [14] X. Lu, W. Wang, Z. Su, S. Liu, and H. Zheng, “Phosphor particle spatial patterning for high angular color uniformity LED packaging through selective curing and settling,” in *2019 20th International Conference on Electronic Packaging Technology (ICEPT)*, 2019, pp. 1–4. doi: 10.1109/ICEPT47577.2019.245234.
- [15] C.-N. Wang, N. T. Thu Khanh, and N. D. Q. Anh, “Improving the correlated color temperature uniformity of multi-chip white LEDs by  $SiO_2$  scatters,” in *2015 International Symposium on Next-Generation Electronics (ISNE)*, 2015, pp. 1–4. doi: 10.1109/ISNE.2015.7131963.
- [16] H. Kumar, S. Gupta, and K. S. Venkatesh, “Resolving focal plane ambiguity using chromatic aberration and color uniformity principle,” in *2018 IEEE 23rd International Conference on Digital Signal Processing (DSP)*, Nov. 2018, pp. 1–5. doi: 10.1109/ICDSP.2018.8631644.
- [17] Z. Tain, J. C. C. Lo, S. W. R. Lee, F. Yun, and R. Sun, “Investigation of the influence of Ag reflective layer on the correlated color temperature and the angular color uniformity of LED with conformal phosphor coating,” in *2015 16th International Conference on Electronic Packaging Technology (ICEPT)*, 2015, pp. 830–834. doi: 10.1109/ICEPT.2015.7236709.
- [18] X. Huang and J. Shi, “A study on the stability and uniformity of LCD,” in *2008 International Conference on Computer Science and Software Engineering*, 2008, pp. 282–285. doi: 10.1109/CSSE.2008.607.
- [19] H. Miyazaki and K. Kamei, “Measurement and analysis of color CRT screen uniformity,” in *Conference Record of the 1988 International Display Research Conference*, 1988, pp. 129–132. doi: 10.1109/DISPL.1988.11292.
- [20] V. Shalamanov, K. Simeonov, and N. Yaneva, “Examination of the dynamic variation of the color homogeneity of the emitted light from a linear LED luminaire with a dynamic color adjustment of the light,” in *2019 Second Balkan Junior Conference on Lighting (Balkan Light Junior)*, Sep. 2019, pp. 1–4. doi: 10.1109/BLJ.2019.8883579.
- [21] T. Asano, T. Kondo, J. Yao, and W. Liu, “White uniformity evaluation of electronic displays based on S-CIELAB color system,” in *2012 9th France-Japan & 7th Europe-Asia Congress on Mechatronics (MECATRONICS) / 13th Int’l Workshop on Research and Education in Mechatronics (REM)*, Nov. 2012, pp. 205–210. doi: 10.1109/MECATRONICS.2012.6451010.
- [22] S. Takamura and N. Kobayashi, “Practical extension to CIELUV color space to improve uniformity,” in *Proceedings. International Conference on Image Processing*, 2002, vol. 2. doi: 10.1109/ICIP.2002.1039970.
- [23] X. Dong, F. Zheng, and Z. Wang, “Research on color uniformity and seam detection of standard test paper based on machine vision,” in *2021 IEEE 4th Advanced Information Management, Communicates, Electronic and Automation Control Conference (IMCEC)*, Jun. 2021, pp. 1391–1395. doi: 10.1109/IMCEC51613.2021.9482203.
- [24] J. Chen, Z. Tian, Q. Wang, J. Liu, and Y. Mou, “Enhanced color rendering and color uniformity of PiG based WLEDs by using red phosphor lens,” *IEEE Photonics Technology Letters*, vol. 33, no. 10, pp. 471–474, 2021, doi: 10.1109/LPT.2021.3069198.
- [25] B. Shang, B. Xie, X. Yu, Q. Chen, and X. Luo, “An improved substrate structure for high angular color uniformity of white light-emitting diodes,” in *2015 16th International Conference on Electronic Packaging Technology (ICEPT)*, 2015, pp. 1094–1097. doi: 10.1109/ICEPT.2015.7236771.

## BIOGRAPHIES OF AUTHORS



**Thuc Minh Bui**    got his B.S. and M.S. degrees in Electrical Engineering from Ho Chi Minh City University of Technology and Education in 2005 and 2008, respectively, and his Ph.D. degree in electrical engineering at from Yeungnam University in Gyeongsan, Korea, in 2018. He is currently a lecturer at the Faculty of Electrical and Electronics Engineering at Nha Trang University in Nha Trang City, Vietnam. His scientific interests include control theory, power converter, automation, and optical science with applications to industry and the environment. He can be contacted at minhb@ntu.edu.vn.



**My Hanh Nguyen Thi**    received a Bachelor of Physics from A Giang University, Vietnam, Master of Theoretical Physics and Mathematical Physics, Hanoi National University of Education, Vietnam. Currently, she is a lecturer at the Faculty of Mechanical Engineering, Industrial University of Ho Chi Minh City, Vietnam. Her research interests are Theoretical Physics and Mathematical Physics. She can be contacted at [nguyenthimyanh@iuh.edu.vn](mailto:nguyenthimyanh@iuh.edu.vn).



**Nguyen Doan Quoc Anh**    was born in Khanh Hoa province, Vietnam. He has been working at the Faculty of Electrical and Electronics Engineering, Ton Duc Thang University. Quoc Anh received his Ph.D. degree from National Kaohsiung University of Science and Technology, Taiwan in 2014. His research interest is optoelectronics. He can be contacted at [nguyendoanquocanh@tdtu.edu.vn](mailto:nguyendoanquocanh@tdtu.edu.vn).



**Nguyen Le Thai**    received his B.S. in Electronic engineering from Danang University of Science and Technology, Vietnam, in 2003, M.S. in Electronic Engineering from Posts and Telecommunications Institute of Technology, Ho Chi Minh, Vietnam, in 2011 and Ph.D. degree of Mechatronics Engineering from Kunming University of Science and Technology, China, in 2016. He is currently with the Nguyen Tat Thanh University, Ho Chi Minh City, Vietnam. His research interests include renewable energy, optimisation techniques, robust adaptive control, and signal processing. He can be contacted at [nlthai@nttu.edu.vn](mailto:nlthai@nttu.edu.vn).